

TITLE PAGE

1
2
3
4
5
6
7
8
9
10
11
12
13
14
15
16
17
18
19
20
21
22
23
24
25

- i. Title:**
The universal imprint of oxygen isotopes can track the origins of seafood
Alternative: Evaluating biomineral oxygen isoscapes for universal seafood provenance
- ii. Running title:**
Oxygen isoscapes for seafood provenance
- iii. Author's names**
Jasmin C. Martino^{1,2*}, Clive N. Trueman³, Debashish Mazumder², Jagoda Crawford², Zoë A. Doubleday^{1*}
- iv. Contact details of corresponding authors:**
Jasmin.Martino@ansto.gov.au, Zoe.Doubleday@unisa.edu.au
- v. The author's institutional affiliations**
¹ MARIS labs, Future Industries Institute, University of South Australia, South Australia 5095, Australia
² Australian Nuclear Science and Technology Organisation (ANSTO), Sydney, Australia.
³ Ocean and Earth Science, University of Southampton, Southampton SO143ZH, UK

ABSTRACT

26

27 Identifying the provenance of seafood is key to helping authorities combat seafood fraud, but
28 current tools are predominantly applied and developed on a species-specific basis. This study
29 investigates how multiple marine taxa could be geolocated at global scales by exploiting stable
30 oxygen isotope compositions in carbonate biominerals ($\delta^{18}\text{O}_{\text{biomin}}$), where we expect to see
31 universally-expressed and predictable spatial variation in $\delta^{18}\text{O}_{\text{biomin}}$ values across taxa. We
32 constructed global ocean isoscapes of predicted $\delta^{18}\text{O}_{\text{biomin}}$ values specific to fish (otoliths),
33 cephalopod (statoliths) and shellfish (shells), and a fourth combined “universal” isoscape, and
34 tested their capacity to predict variations in $\delta^{18}\text{O}_{\text{biomin}}$ values among known-origin samples.
35 High correspondence between isoscape-predicted $\delta^{18}\text{O}_{\text{biomin}}$ values and a compiled database
36 of measured, geo-referenced values (3954 datapoints representing 68 species) indicated that
37 this $\delta^{18}\text{O}_{\text{biomin}}$ approach works well, particularly in regions with highly-resolved projections of
38 seawater $\delta^{18}\text{O}$ composition. The universal isoscape showed similar accuracy compared to
39 taxon-specific isoscapes when predicting $\delta^{18}\text{O}_{\text{biomin}}$ values, demonstrating exciting potential for
40 universal provenance applications. We tested the universal framework on a case study region,
41 with machine learning models used to infer sample origins between regions of divergent
42 climates (Tropical Asia vs Temperate Australasia) and similar climates (Temperate Asia vs
43 Temperate Australasia). Classification accuracy averaged 75.3% between divergent regions
44 and 66% between similar regions. However, when endothermic tuna species were removed
45 from the analyses, accuracy increased up to 90% between divergent regions. This study is a
46 first step towards developing universal chemical markers to support a more inclusive and
47 global approach to verifying provenance of seafood.

48

49 **Highlights:**

- 50 • Universal chemical markers investigated for seafood provenance applications
- 51 • Global ocean oxygen isoscapes were constructed and tested
- 52 • Isoscape models accurately identified multiple taxa to geographical origins
- 53 • First steps towards a more inclusive and global provenance approach

54

55 **Keywords:**

56 Authentication; Biominerals; Fingerprinting; Global model; Isoscape; Provenance

57

58 **Table of contents:**

1. Introduction
2. Materials and methods
 - 2.1. Development of isoscapes
 - 2.2. Testing of isoscapes
 - 2.3. Case study: Assessing isoscape performance for seafood geolocation across Asia and Australia
3. Results
 - 3.1. Development of isoscapes
 - 3.2. Testing of isoscapes
 - 3.3. Case study: Assessing isoscape performance for seafood geolocation across Asia and Australia
4. Discussion
 - 4.1. Conclusions
5. Tables
6. Figures
7. References

59

1. INTRODUCTION

60
61
62
63
64
65
66
67
68
69
70
71
72
73
74
75
76
77
78
79
80
81
82
83
84
85

A healthy and sustainable food system is underpinned by knowing where food comes from, and how it is produced. However, wild-caught seafood is a hard-to-monitor shared resource, and seafood supply chains are often opaque and complex (Fox et al., 2018; Kittinger et al., 2017), which in turn makes seafood particularly vulnerable to fraud. Provenance fraud occurs when consumers or businesses are intentionally deceived about where seafood is caught or its production method, with products often substituted with lower-quality, lower-value versions, or from locations with fewer regulations regarding sustainability or ethics concerns. Such substitution threatens our food system by risking sustainability, safety, and consumer confidence (Lindley, 2020; van Ruth et al., 2017). Provenance fraud can lead to over-exploitation of stocks, which undermines the long-term sustainability of fisheries, the balance of marine ecosystems, and ultimately, harms seafood businesses that rely on these resources (Jacquet & Pauly, 2008; Kompas et al., 2010). Substitute seafood products can also have safety and health implications for consumers, by containing hidden pathogens, banned antibiotics, unlisted allergens or reduced nutrient profiles (Gopi et al., 2019). While many factors influence fisheries sustainability, validating the provenance of seafood empowers authorities to combat seafood fraud and ensures consumers can make an informed choice about the seafood they eat.

The provenance of food can be authenticated using a range of techniques, including DNA profiling (Calosso et al., 2020; Rasmussen & Morrissey, 2008), paper-based and digital tracing, such as blockchain (Howson, 2020), and chemical profiling (Duarte et al., 2022; Martino et al., 2022). While chemical approaches for provenance testing are well-established in terrestrial food forensics, uptake in the aquatic food industry has been slower but is increasingly indicated to have wide potential (Gopi et al., 2019). Natural chemical tracers within seafood tissues can be effective at identifying geographical origins as they are carried

86 unaltered within the product itself and are difficult to falsify. However, existing provenance
87 tools can be prohibitive for many seafoods due to the high cost of developing reference
88 datasets, which are typically optimised for specific species, regions, or supply chains (Kelly et
89 al., 2005). Reference databases are more commonly adopted as standard practise in
90 terrestrial food systems as land-owning producers have more economic incentive to
91 characterise and protect produce originating from land they own (e.g. Monahan et al., 2018;
92 Soares et al., 2017). In marine systems with common access to waters and migratory species,
93 there is less financial incentive for producers to fund chemical or genetic characterisation of
94 specific geographic areas. Furthermore, small-scale fisheries comprise an estimated 70% of
95 the total world catch (Kolding et al., 2014), with many targeting low value stocks, operated by
96 independent fishers with no access to forensic tools, and in exploited waters of developing
97 countries. Traceability methods that rely on development and maintenance of cost-intensive
98 fishery-specific datasets are thus largely inaccessible to these producers. Therefore, a shared
99 provenance system capitalising on consistent inherent properties across taxa could ease the
100 burden of species-specific, cost-prohibitive provenance systems, and improve accessibility of
101 seafood provenance for lower-income regions, smaller industries, or lower-value seafood
102 species.

103 A shared provenance system could be developed using *universal* chemical markers.
104 Here, we define a universal chemical marker as having predictable spatial variation coupled
105 with common expression among taxa (Doubleday et al. in review). Essentially, a universal
106 marker is primarily influenced by the environment whilst species-specific modifications of the
107 environmental signal (e.g. physiological 'vital effects' that vary across taxa) are minimal, so
108 that different taxa living in the same region would share a common chemical value in their
109 tissues. The stable isotope composition of oxygen in calcium carbonate (CaCO_3) biominerals
110 (expressed as $\delta^{18}\text{O}_{\text{biomin}}$ values) has such properties and is a promising candidate for universal
111 provenance applications across broad geographic scales (100s to 1000s km). Oxygen is
112 incorporated into marine animals from seawater with an isotopic composition ($\delta^{18}\text{O}_{\text{water}}$) that is

113 relatively constrained and predominantly varies as a function of salinity, water mass identity,
114 and surface evaporation rate (Craig & Gordon, 1965). In general, typically lower $\delta^{18}\text{O}_{\text{water}}$
115 values are found in higher latitudes due to discharge of river water and glacial meltwater with
116 low $\delta^{18}\text{O}$ values, and higher $\delta^{18}\text{O}_{\text{water}}$ values are observed in highly evaporative regions, such
117 as some sub-tropical zones (Conroy et al., 2014; Singh et al., 2010; Voelker et al., 2015).
118 Global compilations of seawater $\delta^{18}\text{O}_{\text{water}}$ values have been constructed (LeGrande & Schmidt,
119 2006), further constraining region-specific relationships between $\delta^{18}\text{O}_{\text{water}}$ values and salinity.
120 Consequently, with high resolution salinity data, $\delta^{18}\text{O}_{\text{water}}$ values can be predicted with
121 confidence on global scales. During biomineralisation, oxygen isotopes are fractionated with
122 preferential incorporation of the lighter ^{16}O isotope. The extent of this fractionation depends
123 on the temperature of mineral growth (Kalish, 1991; Kim et al., 2007), which in marine
124 ectothermic organisms is the ambient seawater temperature. The form of the temperature-
125 dependent equation of $\delta^{18}\text{O}_{\text{biomin}}$ has been investigated extensively as it forms the basis for
126 palaeotemperature reconstructions (Zachos et al., 1994), with $\delta^{18}\text{O}_{\text{biomin}}$ thermometry
127 equations experimentally derived for a range of fish (e.g. Geffen, 2012; Godiksen et al., 2010;
128 Høie et al., 2004; Sakamoto et al., 2019; Thorrold et al., 1997), gastropod and bivalve species
129 (e.g. Grossman & Ku, 1986; Nishida et al., 2015; Owen et al., 2008; Wanamaker Jr et al.,
130 2007), as well as a single cephalopod species (Chung et al., 2020). However, there remains
131 some debate on whether $\delta^{18}\text{O}_{\text{biomin}}$ values reflect ambient temperatures in fish with regional
132 endothermy, such as some shark and tuna species (Graham & Dickson, 2004; Hane et al.,
133 2020).

134 Given global scale predictions of $\delta^{18}\text{O}_{\text{water}}$ values and temperatures in the ocean
135 alongside the well-established biogeochemical relationships, it is possible to create spatial
136 models (“isoscapes”) of predicted $\delta^{18}\text{O}_{\text{biomin}}$ values in tissues of marine animals (Trueman et
137 al., 2012). Isoscapes are typically displayed as spatial maps of isotopic distributions and can
138 be used to determine the most likely geographic origins of an organism by matching the
139 isotopic composition of its tissue to area(s) on the isoscape with similar values. Isoscapes

140 have been used in both terrestrial and aquatic ecology to investigate animal movements and
141 environmental histories (Artetxe-Arrate et al., 2021; Pearson et al., 2020; Trueman & Glew,
142 2019), but have had little application in marine food provenance.

143 Here, we propose that globally-predicted, universal $\delta^{18}\text{O}_{\text{biomin}}$ markers are effective
144 indicators of provenance for multiple marine taxa. Our taxa of interest included teleost fish,
145 bivalves and gastropods (hereafter called shellfish), and coleoid cephalopods, which are
146 critical components of the world's seafood supply. Our specific objectives were to 1) develop
147 and compare three global ocean isoscapes of predicted $\delta^{18}\text{O}_{\text{biomin}}$ values in fish, cephalopods
148 and shellfish, with a fourth "universal" multi-taxa isoscape, 2) test predicted isoscape-derived
149 $\delta^{18}\text{O}_{\text{biomin}}$ values through comparing against a global database of measured, geo-referenced
150 $\delta^{18}\text{O}_{\text{biomin}}$ values, and evaluate predictors of variation in residuals; and 3) in a case study,
151 assess the isoscape performance for geolocating multiple taxa between regions with divergent
152 (Tropical Asia vs Temperate Australasia) or similar (Temperate Asia vs Temperate
153 Australasia) climatic profiles.

154

CONFIDENTIAL

2. MATERIALS AND METHODS

155

156

157 2.1 Development of isoscapes

158 Mechanistically-predicted global ocean isoscapes of $\delta^{18}\text{O}_{\text{biomin}}$ values were constructed using
159 environmental datasets and established biogeochemical relationships from the literature.
160 Three isoscapes were built specific to aragonitic calcium carbonate (CaCO_3) biominerals of
161 fish (otoliths), shellfish (exoskeleton shells of bivalve and gastropod molluscs), and
162 cephalopods (statoliths). A fourth “universal” isoscape was then created via an average of the
163 taxon-specific isoscapes. All modelling and analysis was done in R (R Development Core
164 Team 2008), with isoscapes developed using R packages raster (Hijmans et al., 2015), gstat
165 (Pebesma, 2004), and rasterVis (Lamigueiro et al., 2022; Liaw & Wiener, 2002).

166 $\delta^{18}\text{O}_{\text{biomin}}$ values were predicted from literature datasets of sea surface temperature and
167 $\delta^{18}\text{O}_{\text{water}}$ values. Sea surface temperatures ($^{\circ}\text{C}$, 0.05° resolution) representing a depth of
168 20 cm were taken as weekly intervals from the ESA Sea Surface Temperature Climate
169 Change Initiative through the Copernicus E.U. Copernicus Marine Service Information
170 (Merchant et al., 2019). Data across a 4-year period (February 2017 – January 2021) were
171 extracted and averaged across this period and transformed to $1^{\circ} \times 1^{\circ}$ resolution using bilinear
172 resampling. A global gridded data set of $\delta^{18}\text{O}_{\text{water}}$ values (‰, $1^{\circ} \times 1^{\circ}$ resolution) were also
173 obtained (LeGrande and Schmidt 2006). This gridded data set was constructed from direct
174 $\delta^{18}\text{O}_{\text{water}}$ measurements combined with estimates calculated from regional $\delta^{18}\text{O}_{\text{water}}$ to salinity
175 relationships in areas of sparse data.

176 The terms used in the thermometry equations for predicting the $\delta^{18}\text{O}$ values in biominerals
177 included: $\delta^{18}\text{O}_{\text{biomin.VPDB}}$ indicating the predicted values of $\delta^{18}\text{O}$ in carbonates reported relative
178 to Vienna Pee Dee Belemnite (VPDB), $\delta^{18}\text{O}_{\text{water.VSMOW}}$ indicating the $\delta^{18}\text{O}$ of seawater relative
179 to Vienna Standard Mean Ocean Water (VSMOW), and SST indicating the sea surface
180 temperature in Celsius ($^{\circ}\text{C}$).

181

182 A single experimentally-derived thermometry equation for statoliths of cephalopods has been
183 published and was used to predict $\delta^{18}\text{O}$ values in statoliths (Chung et al., 2020):

$$184 \quad \delta^{18}\text{O}_{\text{biomin.VPDB}} = -0.20(\pm 0.005) \times \text{SST}(\text{°C}) + 2.88 (\pm 0.14) + \delta^{18}\text{O}_{\text{water.VSMOW}}$$

185

Equation 1

186 A range of thermometry equations for otoliths of teleost fish species have been experimentally
187 validated (Table S1). As we aimed to construct an isoscape that could be widely applied
188 across species, an averaged thermometry equation was derived from these published
189 experimental studies (Geffen, 2012; Høie et al., 2004; Kitagawa et al., 2013; Nakamura et al.,
190 2020; Radtke et al., 1996; Sakamoto et al., 2017; Thorrold et al., 1997). The selection aimed
191 to include a range of functional groups of marine fish and included those with equations in
192 suitable algebraic forms. The averaged thermometry equation used to predict $\delta^{18}\text{O}$ values in
193 otoliths was:

$$194 \quad \delta^{18}\text{O}_{\text{biomin.VPDB}} = -0.2143 (\pm 0.012) \times \text{SST}(\text{°C}) + 4.056 (\pm 0.28) + \delta^{18}\text{O}_{\text{water.VSMOW}}$$

195

Equation 2

196 For shellfish, we first compared the suitability of two equation forms, an averaged thermometry
197 equation averaged from validated aragonitic shells and one of the most widely used
198 thermometry equation for shellfish, the biogenic aragonite calibration from Grossman and Ku
199 (1986) which is derived from a range of species. The Grossman and Ku model was
200 subsequently chosen due to lower residual sum of squares when comparing predicted
201 $\delta^{18}\text{O}_{\text{biomin}}$ values against measured values (see Supplementary Information, Figure S1). The
202 form of the Grossman and Ku equation used was modified by Hudson and Anderson (1989),
203 with a 0.38 ‰ offset applied to compensate for differences in acid fractionation factors of
204 calcite and aragonite (Caldarescu et al., 2021). The equation used to predict $\delta^{18}\text{O}$ values in
205 shells was:

$$\delta^{18}\text{O}_{\text{biomin.VPDB}} = \frac{\text{SST}(\text{°C}) - 19.7}{-4.34} + \delta^{18}\text{O}_{\text{water.VSMOW}} - 0.38$$

207 Equation 3

208 Predicted $\delta^{18}\text{O}_{\text{biomin}}$ values were calculated for each 1° by 1° cell, and plotted as a global map
209 using ggplot2 in R (Wickham, 2011). The universal biomineral isoscape was constructed by
210 averaging the predicted $\delta^{18}\text{O}_{\text{biomin}}$ values per cell across the three taxon-specific isoscapes.

211

212 **2.2 Testing of isoscapes**

213 To test the correspondence between the isoscape models and measured $\delta^{18}\text{O}_{\text{biomin}}$ values, we
214 used an expanded version of a previously compiled database of $\delta^{18}\text{O}_{\text{biomin}}$ values in fish,
215 coleoid cephalopods and shellfish, that were collected alongside geographical harvest
216 coordinates (Doubleday et al., in review). The database comprised of published $\delta^{18}\text{O}_{\text{biomin}}$
217 values represented as means per species per harvest location derived from the literature
218 (1995 to 2021), as well as a smaller number of unpublished values, provided by the authors.
219 This database was expanded for the current project through extracting individual datapoints
220 of $\delta^{18}\text{O}_{\text{biomin}}$ from publications, where available, and represented wild-caught, wholly marine,
221 subtidal taxa collected from depths of less than 500 m. However, due to the spatial resolution
222 of the isoscapes along coastlines, some datapoints from coastal zones were ultimately
223 excluded. As such, 3954 datapoints derived from 68 species were ultimately used to represent
224 the measured values. The database represents data from both the whole carbonate structure
225 or the period corresponding to the area of capture (i.e. marginal increment of otoliths of
226 migratory species) where appropriate. To assess regional-specific trends in the isoscapes,
227 measured values were assigned to groups corresponding to 10 ocean ecoregions – Arctic,
228 Central Indo-Pacific, Mediterranean, Temperate Australasia, Temperate Northern Atlantic,
229 Temperate Northern Pacific, Temperate South America, Tropical Atlantic, Tropical Eastern
230 Pacific, and Western Eastern Pacific (Spalding et al., 2007). As one of the main objectives of

231 this study is the universal and practical application of the isoscape, shellfish species that had
232 calcitic shells, aragonitic shells, or shells that were a mixture of both calcite and aragonite
233 were included. All other measured values of carbonates represented aragonitic structures.

234 For each coordinate of the measured database values, a matching predicted $\delta^{18}\text{O}_{\text{biomin}}$
235 value was extracted from the isoscapes as a 1° by 1° cell mean around the coordinate of
236 capture. Residuals (differences) between the measured $\delta^{18}\text{O}_{\text{biomin}}$ values from the database
237 and predicted values from the isoscapes were calculated to investigate discrepancies between
238 model-predicted and measured values. Global maps of residuals were constructed using
239 inverse distance weighting interpolation.

240 To investigate sources of variation in discrepancies between model-predicted and
241 measured $\delta^{18}\text{O}_{\text{biomin}}$ values, linear models were used to explore partitioning of the residuals
242 among potential predictor variables. Predictors included ocean ecoregion, taxa, latitude,
243 longitude and year of capture. For shellfish models, the CaCO_3 polymorph (aragonite, calcite,
244 or combined) was also included as a predictor. Model residuals were checked for normal
245 distribution and homogeneity of variance, while collinearity of predictors was assessed using
246 variance inflation factors below >2.5 . Due to geographical predictors being highly collinear,
247 two models were compared either excluding longitude and latitude or excluding ocean region
248 using Akaike's information criterion corrected for small sample sizes (AICc; Burnham and
249 Anderson 2004). Relative importance weights were derived to assess the proportional
250 contribution of each predictor to the variability of the dependent value (Grömping, 2006).
251 Estimated Marginal Means derived from the optimal model was then used to investigate
252 whether the residuals differed significantly ($p < 0.05$) between ocean ecoregion, taxa, and
253 polymorph after accounting for the influence of all other predictors using package emmeans
254 (Lenth et al., 2018). Pairwise comparisons were conducted using a Tukey adjustment.
255 Subsequently, otolith isoscape-derived values were re-run in a separate linear model to
256 assess if residuals for endothermic tuna species (*Thunnus* sp.) were significantly different to
257 ectothermic fish. The species in our dataset we tested were albacore tuna (*Thunnus alalunga*),

258 Atlantic bluefin tuna (*Thunnus thynnus*), Pacific bluefin tuna (*Thunnus orientalis*), southern
259 bluefin tuna (*Thunnus maccoyii*), and yellowfin tuna (*Thunnus albacares*).

260

261 **2.3 Case study: Assessing isoscape performance for seafood geolocation** 262 **across Asia and Australia**

263 A case study was conducted to assess the efficacy of using $\delta^{18}\text{O}_{\text{biomin}}$ values to
264 geolocate seafood to geographical origins in a real-world scenario, and to compare accuracy
265 between regions of divergent or similar climatic profiles and latitudes. Regions in eastern Asia
266 and Australasia were selected as they represent markets with high levels of seafood trade and
267 suitable environmental profiles. “Temperate Asia” and “Temperate Australasia” were selected
268 to represent similar climatic profiles and latitudes, while “Tropical Asia” was selected to
269 represent a divergent climate profile from the temperate regions (Figure 5). A machine learning
270 approach using random forest was used to classify region of origin of measured $\delta^{18}\text{O}_{\text{biomin}}$
271 values harvested within the boundaries of study regions. The random forest algorithm
272 determines classifications using the aggregated results of an ensemble of individual
273 classification and regression trees built using a random bootstrap of the data. Random forest
274 models was built using R package randomForest (Liaw & Wiener, 2002) for each taxon-
275 specific isoscape and the universal biomineral isoscape. Grid values of $\delta^{18}\text{O}_{\text{biomin}}$ representing
276 1° mean latitude and longitude steps within regions of interest (Temperate Australasia,
277 Temperate Asia, and Tropical Asia) were extracted from each isoscape and then used to train
278 each model with k-fold cross-validation incorporated. Out-of-bag (OOB) errors were derived
279 to measure the predictive capacity of the trained model using bootstrap aggregating, whilst
280 Cohen's kappa coefficient was calculated as an additional metric of classifier performance.
281 Subsequently, random forest models predicted the region of origin of measured $\delta^{18}\text{O}_{\text{biomin}}$
282 values with accuracies derived by comparing the resulting matrix of class probabilities to the
283 known regional classifications. To assess if model accuracies were improved with the

284 exclusion of endothermic tuna, we re-ran the universal and otolith-isoscape models without
285 *Thunnus* sp.

CONFIDENTIAL

286

3. RESULTS

287 3.1 Development of isoscapes

288 Isoscapes of mechanistically-predicted $\delta^{18}\text{O}_{\text{biomin}}$ values were successfully constructed
289 for fish, cephalopod, and shellfish, as well as a universal average isoscape (Figure 1). Global
290 trends were similar among taxa, and at global scales spatial variance was dominated by
291 thermal effects, with more positive $\delta^{18}\text{O}_{\text{biomin}}$ values closer to the poles and more negative
292 $\delta^{18}\text{O}_{\text{biomin}}$ values closer to the equator (Figures S2B, S3).

293 3.2 Testing of isoscapes

294 The trends in residuals between predicted values derived from the isoscape model and
295 measured $\delta^{18}\text{O}_{\text{biomin}}$ values from the database provided an understanding of the variation
296 between regions and taxa. The measured $\delta^{18}\text{O}_{\text{biomin}}$ values spanned between -5.3 to 3.9‰,
297 corresponding well with the isoscape ranges (Figure 2A). Although residual sum of squares
298 were similar between the universal and taxon-specific isoscapes when separating out the taxa
299 (± 1), the universal isoscape produced lower average residuals for statoliths (1.2 vs 1.6 ‰) and
300 otoliths (-0.07 vs -0.4 ‰), but higher residuals for shells (0.5 vs 0.4 ‰) (Figure 2B, Figure 3).

301 Linear regressions uncovered the key influences on the residuals of $\delta^{18}\text{O}_{\text{biomin}}$ values.
302 The linear model derived from the universal isoscape explained 41.0% of the variance ($p <$
303 0.001). Ocean region was the dominant predictor, responsible for 82.2% of the model
304 variance. This regional variation was also demonstrated through significant differences ($p <$
305 0.05) between many regions. The estimated marginal means of residuals were the most
306 negative in the Arctic (-0.96 ‰) and Mediterranean (-0.73 ‰), whilst the most positive
307 estimated marginal means were found in Temperate South America (1.32 ‰) and the Central
308 Indo-Pacific (1.49 ‰) (Figure 4). The estimated marginal means of residuals in the Temperate
309 Northern Atlantic (0.09 ‰) had values closest to 0, indicating the predicted values closely
310 aligned with the measured values. Taxon was responsible for 15.2% of the model variance.
311 Cephalopods (0.75 ‰) and shellfish (0.8 ‰) had similar positive estimated marginal means of

312 residuals, whilst the estimated marginal mean for the group 'fish' was significantly lower (-
313 0.06‰). Polymorph was responsible for 1.9% of the variance but was not significantly different
314 between aragonite, calcite, or combined mixes of the two. Year of capture was responsible for
315 0.5% variation but was also not significant.

316 The linear model assessing the taxon-specific isoscapes explained 46.7% of the
317 variance (R^2) of the residuals ($p < 0.001$). Compared to the universal model, taxon was a more
318 dominant influence in these individual isoscapes. While ocean region remained the dominant
319 influence of variation at 66.3%, taxon was responsible for 31.0% of variance in residuals,
320 polymorph 1.9%, and 0.6% to year of capture. The estimated marginal means of the residuals
321 for ocean regions largely aligned with those described for the universal model, however the
322 estimated marginal means for taxon were significantly different between all groups. Compared
323 to the universal models, estimated marginal means of residuals were closer to zero (0.62 vs
324 0.8 ‰) for the shell isoscape, more negative but further from zero (-0.39 vs -0.06 ‰) for the
325 otolith isoscape, and more positive but similarly further from zero (1.25 vs 0.75 ‰) for the
326 statolith isoscape. Like the universe isoscape regression models, the polymorph and year of
327 capture did not significantly influence residuals.

328 **3.3 Case study: Assessing isoscape performance for seafood geolocation across Asia** 329 **and Australia**

330 In the case study, measured test samples ($n = 1097$, species = 16) were classified back to
331 geographical source between regions of both divergent (Tropical Asia) and similar (Temperate
332 Asia, Temperate Australasia) climatic profiles and latitudes (Figure 5). Lower values of
333 Cohen's kappa coefficients compared to classification accuracies were observed, primarily
334 due to class imbalances. For the universal isoscape model (OOB: 15.6%, Kappa: 0.2) overall
335 accuracy at classifying samples back to region of origin across the three regions was 50.5%
336 (554 out of 1097 samples) (Table 1). Samples could be correctly distinguished between
337 tropical and temperate zones with 72.6% (796 out of 1097 samples) accuracy, but this
338 accuracy rate dropped to 63.4% (434 out of 684 samples) when attempting to distinguish

339 between the two temperate zones (Kappa: 0.56). Across the taxon-specific models (mean
340 OOB 13.5%, Kappa: 0.17), mean overall accuracy across the three regions was 54.4% (Table
341 1). For the otolith isoscape model, samples could be distinguished between tropical and
342 temperate zones with a 58.5% (304 out of 520 samples) success rate. When discriminating
343 between the two temperate zones, accuracy was 84.2% (107 out of 127 samples; Kappa:
344 0.55). For the statolith isoscape model, samples were distinguished between tropical and
345 temperate zones with a 70% (28 out of 40 samples) success rate, and between the two
346 temperate zones with 50% (10 out of 20 samples) correctly distinguished (Kappa: 0.53). For
347 the shell isoscape model, no measured Tropical Asia samples from the database were
348 available so only temperate samples were tested against the model. These included
349 temperate samples were 100% correctly classified as temperate rather than tropical (537 out
350 of 537 samples), whilst 62% (333 out of 537 samples) of these samples were correctly
351 distinguished between the two temperate zones (Kappa: 0.5).

352 The tuna species were found to influence both the linear models and accuracy of the
353 classification models. The otolith isoscape linear model that included a *Thunnus sp.* predictor
354 variable showed that the estimated marginal means of residuals between predicted and
355 measured $\delta^{18}\text{O}_{\text{biomin}}$ values were significantly more negative (-1.08 ‰) for the tuna group than
356 the other teleost fish (0.2 ‰). When the classification models from universal and otolith
357 isoscapes were rerun with *Thunnus* excluded, correct classifications increased when
358 distinguishing between the temperate and tropical zones. The universal model increased from
359 72.6% to 90% (689 out of 766 samples) accuracy, and the otolith model increased from 58.5%
360 to 69.3% (131 out of 189 samples) accuracy. However, excluding *Thunnus* did not alter the
361 classification success between the two temperate zones.

362

4. DISCUSSION

363

364

365 Oxygen isoscapes were successfully applied to track the geographical origins of a
366 broad range of marine species. The universal isoscape was a more accurate predictor of
367 geographic origin than taxon-specific isoscapes for cephalopods and fish, whilst the shell
368 isoscape was a more accurate predictor for shellfish. Classification models developed from
369 isoscapes generally performed best when assigning animals back to their region of origin
370 between test regions with high temperature and latitudinal contrast (i.e., tropical versus
371 temperate waters). Our results indicate that oxygen isoscapes are most powerful for
372 geolocating animals over larger latitudinal gradients (100s to 1000s km), where there are
373 known regional differences in water temperature and salinity. While traceability tools are
374 typically species or supply-chain specific, these results demonstrate the potential of oxygen
375 isotopes for a universal and combined provenance approach for marine animals.

376 The promising implication of the universal isoscape being comparable, and sometimes
377 more accurate, at predicting $\delta^{18}\text{O}_{\text{biomin}}$ than the taxon-specific isoscapes is that it demonstrates
378 suitability for a wide-range of species without the need for prior taxon-specific collation of
379 reference data. This higher accuracy is likely assisted by the averaging of a range of
380 thermometry equations to develop the isoscape. While consistent negative linear relationships
381 are demonstrated between $\delta^{18}\text{O}_{\text{biomin}}$ values and temperature, there are minor species and
382 taxonomy variation in equation coefficients, particularly intercepts (Chung et al., 2020;
383 Kitagawa et al., 2013; Shirai et al., 2018), potentially owing to differences in haemoglobin
384 oxygen-binding affinity, or oxygen sources within body fluids (Macdonald et al., 2020).
385 Differences in experimental set-up, such as experimental temperature range, alongside
386 measurement and statistical errors, may also have had a minor influence on equation
387 coefficients between species. Whilst there are examples of isoscapes being effectively
388 developed and applied using a thermometry equation validated for a single-species (Artetxe-

389 Arrate et al., 2021; Pearson et al., 2020; Trueman et al., 2012), the idea here is that a
390 combined equation may be more likely to be physiologically-relevant to a randomly chosen
391 species on average. Further testing will help to refine the averaged equation for optimal
392 applications across species and taxa. In particular, most experimental studies validating the
393 relationship between temperature and $\delta^{18}\text{O}_{\text{biomin}}$ values were derived from temperate or sub-
394 arctic temperature ranges and study species (Geffen, 2012; Høie et al., 2004; Radtke et al.,
395 1996), although there are a couple of exceptions (Chung et al., 2020; Kitagawa et al., 2013).
396 It is evident that more experimental research is needed to define thermometry equations
397 specific to tropical species, which would allow for more accurate use of $\delta^{18}\text{O}_{\text{biomin}}$ as a universal
398 proxy.

399 For endothermic fish like tuna our results show that $\delta^{18}\text{O}_{\text{biomin}}$ values need to be applied
400 cautiously. Residuals between measured and predicted $\delta^{18}\text{O}_{\text{biomin}}$ values were significantly
401 more negative for *Thunnus* species in our database compared to the other fish species and
402 subsequently, when these samples were excluded from the classification models, accuracy
403 improved. Many tuna species can elevate their muscle, visceral, and cranial temperatures
404 using counter-current heat exchangers known as retia mirabilia (Graham & Dickson, 2004;
405 Malik et al., 2020). As such, $\delta^{18}\text{O}_{\text{biomin}}$ values could reflect elevated, internal temperatures
406 rather than just environmental temperatures, although it is difficult to consistently predict to
407 what extent as the thermoregulatory ability of tuna can vary with somatic size and ambient
408 ocean temperatures (Kitagawa et al., 2006). While further research is needed to determine
409 the extent that endothermy affects $\delta^{18}\text{O}_{\text{biomin}}$ values for provenance applications, endothermy
410 is a rare phenomenon in fish and is only relevant to tuna, billfish and a small number of shark
411 species (Madigan et al., 2015).

412 The shells of bivalves and gastropods can comprise of either calcite or aragonite
413 polymorphs, or a combination of both, which can influence $\delta^{18}\text{O}_{\text{biomin}}$ – temperature
414 relationships due to differing fractionation factors. However, it was found that this variability in
415 CaCO_3 polymorphs has minimal impact on the accuracy that can be achieved using $\delta^{18}\text{O}_{\text{biomin}}$

416 values as a provenance tool. No significant differences were found in $\delta^{18}\text{O}_{\text{biomin}}$ values between
417 polymorphs in the bivalves and gastropods. While the coefficients of the oxygen thermometry
418 equation vary based on the polymorph, we found that for broader scale provenance purposes
419 the variation in $\delta^{18}\text{O}_{\text{biomin}}$ values due to polymorph type was small compared to spatial
420 variation. This result is backed by a previous field study that found minimal isotopic differences
421 between calcite and aragonite layers in different gastropod and bivalves species growing in
422 the same environment (Lécuyer et al., 2012). While identifying and separating the polymorphs
423 prior to isotopic analysis can be achieved (i.e., using x-ray diffraction and mechanically
424 separating calcite and aragonite layers), this would be a time-consuming and costly process.
425 The consistency of results here between calcite and aragonite structures indicates that for
426 universal applications, where the aim is to save time and effort for industry and research, a
427 combined system is likely optimal.

428 We were also interested in identifying whether universal geolocation is equally
429 applicable across regions. Predictions of $\delta^{18}\text{O}_{\text{biomin}}$ values were most accurate in the
430 Temperate Northern Pacific and Temperate Northern Atlantic regions but least accurate in the
431 Central Indo-Pacific and Temperate South America. This difference in accuracy between
432 regions may stem from the variability in the number of measurements between regions used
433 to derive the gridded data of $\delta^{18}\text{O}_{\text{water}}$ (LeGrande & Schmidt, 2006). While the dataset was
434 developed with a relatively consistent coverage of directly measured $\delta^{18}\text{O}_{\text{water}}$ values in the
435 northern Pacific and northern Atlantic Oceans, areas of sparse coverage are clearly evident
436 such as along the southern coastline of South America and tropical Asia. This insight highlights
437 that isoscape applications work best for regions with highly resolved current projections of
438 $\delta^{18}\text{O}_{\text{water}}$ values. For regions with high residuals, predicted accuracies could be improved
439 through incorporating localised seawater measurements of $\delta^{18}\text{O}_{\text{water}}$, or coupling detailed
440 salinity projections with specific regional $\delta^{18}\text{O}_{\text{water}}$ – salinity relationships.

441 While we demonstrate the promising potential of universal oxygen isoscapes to
442 geolocate seafood, there are current limitations. As the oxygen isoscapes developed here

443 cover fully marine, surface conditions, it is necessary to have a good understanding of the life-
444 history, habitat use, and movement and migratory patterns of the study species, particularly
445 identifying taxa with nearshore, subtidal or estuarine habitats or life stages. It is also possible
446 that for highly migratory species, such as tuna, chemical markers may represent the migratory
447 path rather than harvest location. Using age data alongside targeted sampling of new otolith
448 growth is recommended to isolate $\delta^{18}\text{O}_{\text{biomin}}$ values that represent the harvest location.
449 Moreover, the compiled database of measured geo-referenced samples used to test the
450 isoscape was relatively scarce for offshore, pelagic samples compared to samples from
451 inshore or shelf sea settings (Figure 2A). This is likely driven by coastal marine ecosystems
452 accounting for 95% of the biomass of fisheries catch, likely in part due to easier accessibility
453 and lower costs for fishers, despite covering only 22% of ocean area (Stock et al., 2017). As
454 such, the assignment potential estimates presented should be cautiously applied to species
455 in open ocean. Similarly, our isoscape models represent shallow ocean depths and further
456 investigation is needed to test the accuracy of the approach in deeper water species. However,
457 previous research indicates that predicted $\delta^{18}\text{O}_{\text{biomin}}$ values in otoliths are highly consistent in
458 depths between 0 – 50 m, and while values became more positive in deeper depths, spatially-
459 driven variation in $\delta^{18}\text{O}_{\text{biomin}}$ values still remained dominant (Artetxe-Arrate et al., 2021). Lastly,
460 $\delta^{18}\text{O}_{\text{biomin}}$ approaches are clearly not applicable to seafood taxa that do not possess calcitic or
461 aragonitic tissues. While most seafood taxa have CaCO_3 tissues, sharks and other
462 elasmobranch fish are a key group that do not. However, phosphate and structural carbonate
463 ions within bioapatite of skeletal structures of vertebrate animals are potential targets for
464 applying universal oxygen isotope markers (e.g. Bryant et al., 1996). Furthermore, more
465 research is required on understanding oxygen thermometry relationships in decapod
466 crustaceans, which form a significant component of the seafood supply. Crustacean
467 exoskeletons are mixture of organic matrices, calcite or Mg-calcite, and amorphous
468 polymorphs of calcium carbonate (Luquet, 2012), so oxygen thermometry equations
469 developed for fish and molluscs may not be as accurate.

470 In addition to these taxonomic considerations, the isoscapes presented here are
471 constructed from annual means in temperature and salinity. However, seasonal fluctuations
472 of temperature and salinity can influence $\delta^{18}\text{O}_{\text{biomin}}$ values and the magnitude of this influence
473 would vary between regions. For example, when global $\delta^{18}\text{O}$ values in barnacle calcite were
474 predicted separately for individual seasons, mid-litudinal regions (30° to 60°) with large
475 annual temperature gradients had the largest differences in isotope values (up to $1.9 \pm 0.7 \text{ ‰}$)
476 (Pearson et al., 2020). Conversely, minimal changes in isotopic values were found in the
477 tropics and southern polar regions, where seasonal temperature fluctuations are limited. While
478 in the current study higher residuals were not observed in mid-litudinal zones, addressing
479 season of capture is an area for refinement in future studies. Local variations in time-resolved
480 $\delta^{18}\text{O}_{\text{biomin}}$ values may indeed provide finer-scale assignment potential, particularly for shellfish
481 where high-resolution time-resolved sampling is relatively simple across the shell, and the
482 sessile nature ensures that variation through time is directly linked to local variations in
483 temperature (and possibly salinity).

484 To improve the predictive ability and spatial resolution of $\delta^{18}\text{O}_{\text{biomin}}$ values as a
485 provenance tool, particularly among samples collected from similar latitudes, additional
486 isotopic or elemental layers with universal properties could be introduced to the isoscape. Like
487 $\delta^{18}\text{O}_{\text{biomin}}$ values, complementary universal chemical markers require predictable spatial
488 variation coupled with common expression amongst species. While carbon isotopes ($\delta^{13}\text{C}$) in
489 biominerals are generally analysed concurrently with $\delta^{18}\text{O}$, they are unsuitable in this context
490 as $\delta^{13}\text{C}$ values in seawaters are generally homogenous ($\sim 0 \text{ ‰}$) whilst values in carbonates
491 can vary across individuals due to diet and metabolic influences (Chung et al., 2021; Chung
492 et al., 2019; Martino et al., 2020). In contrast, neodymium isotopes ($^{143}\text{Nd}/^{144}\text{Nd}$ ratios
493 expressed as ϵ_{Nd} values) are indicated to be driven by continental geology and thus exhibit
494 distinct geographic profiles in the ocean with high spatial resolution (Jeandel et al., 2007).
495 Recent research suggests that ϵ_{Nd} values in the soft and hard tissues of bivalve molluscs are
496 highly successful at identifying the origins of individuals across even small spatial scales (10s

497 km) (Saitoh et al., 2018; Tanaka et al., 2022; Zhao et al., 2019). Concentrations of barium
498 ratioed to calcium (Ba/Ca) could also be effective for provenance as biomineral signatures
499 reflect seawater values (Bath et al., 2000; Walther & Thorrold, 2006), and are little affected by
500 individual life-history, such as physiology or diet (Grammer et al., 2017; Hüseyin et al., 2021;
501 Martino et al., 2021). However, significant work first needs to be undertaken to estimate spatial
502 variations in these potential universal markers. Alternatively, chemical markers could be used
503 in conjunction with taxa-specific provenance methods, such as DNA markers or fatty acid
504 profiling. While using multiple methods and biomarkers to infer the marine food provenance
505 can strengthen the accuracy and precision of provenance assignment (Cazelles et al., 2021),
506 the additional time and financial costs need to balance with likely benefit. For example, a
507 recent meta-analysis of provenance testing using DNA and isotopic markers, found that for 3
508 of the 63 teleost fish species investigated a combined DNA-isotope approach reduced the
509 chance of misassignment (Cusa et al., 2022). The study thus concluded that using both DNA
510 and isotopes would be likely most useful where the provenance regions of interest include
511 water bodies that are isotopically similar (i.e. between Temperate Asia and Australasia in this
512 study) or where populations that are genetically similar.

513 Chemical markers are used extensively in ecological and fisheries applications (e.g.,
514 defining stock structure or fishery management units), but their application to address seafood
515 provenance fraud, as well as their integration into associated management and policy
516 decisions, is scarce (Camin et al., 2016; Cusa et al., 2021). This is also the case for DNA-
517 based approaches, whereby uptake by managers and policymakers for seafood
518 authentication has stagnated (Bernatchez et al., 2017; Cusa et al., 2021; Martinsohn et al.,
519 2019). For DNA-based approaches, roadblocks to uptake include limited awareness on the
520 true costs and benefits of DNA analyses (e.g. perceived analytical costs versus value of
521 confiscated catches and associated fines), as well as poor communication between scientists,
522 managers, and policymakers about the relevant methods (Bernatchez et al., 2017; Martinsohn
523 et al., 2019). We suggest that awareness and communication about chemical markers, and

524 the efficiencies that could be achieved using a universal approach, is also key to uptake,
525 alongside demonstrating tangible outcomes. For instance, universal markers could be applied
526 to distinguish multiple marine taxa from protected designations of origin (PDO), which has
527 been successfully achieved using a species-specific marker approach, e.g. the authentication
528 of mussels from Galicia (Costas-Rodríguez et al., 2010), or between key trade locations, as
529 demonstrated here between south-east Asia and Australia. Furthermore, a universal marker
530 approach negates the need for developing time-consuming reference databases for different
531 species and target regions (Li et al., 2016), which is a drawback of current chemical marker
532 methods and a roadblock to uptake by industry (Camin et al., 2016). However, incentives to
533 use provenance technology to support sustainable seafood practices do vary, with seafood
534 labelling policies and regulations being vastly different among jurisdictions (Lindley, 2021).
535 Involvement from PDO protection consortia, producers' associations, or eco-certification
536 organisations can drive real world applications (Camin et al., 2016). For example, the Marine
537 Stewardship Council used DNA barcoding to verify the species of 100s of sampled seafood
538 products collected from multiple countries (Barendse et al., 2019). Chemical markers,
539 alongside DNA-based approaches, are well regarded methods for delineating population
540 structure for fisheries management applications, therefore we are optimistic the universal
541 approach outlined here could be achieved for seafood provenance applications through ongoing
542 communication with stakeholders and a coordinated international approach to method
543 development.

544

545 **4.1 Conclusions**

546 Here, we demonstrate how universal chemical markers and isoscape mapping approaches
547 can successfully geolocate a diverse range of seafood back to the region of origin. These
548 techniques have the potential to change the way we verify the provenance of seafood on a
549 more unified, global, and equitable scale. Oxygen isotope compositions in biominerals provide
550 an accurate tool for geolocating samples across large latitudinal and thermal gradients, but

551 could be augmented with additional isotopic and elemental layers or species-specific
552 approaches (e.g. DNA markers) to improve the spatial resolution and precision of the
553 framework. Furthermore, biomineral structures have several key advantages over soft tissues
554 for seafood provenance applications: they permanently retain lifetime chemical fingerprints;
555 do not decay; are often discarded or low-valued by the seafood industry; and are commonly
556 routinely retained for other purposes, such as aging of stocks (e.g., otoliths). Additionally, we
557 can draw upon the extensive ecological and fisheries literature developed using chemical
558 profiling of biominerals for reconstructing environmental or movement histories. Validating the
559 provenance of seafood products on a global scale is a large and complex undertaking due to
560 the diversity of species, fisheries, and socio-economic drivers. Here, we present a more
561 universal method that is applicable to multiple taxa and seafood products and could provide
562 access to provenance for smaller or lower-income producers, and to species with lower
563 commercial value. Provenance fraud continues to be a significant issue that threatens food
564 security, equitable access to resources, food safety, and consumer confidence in seafood
565 products. The development of universal chemical markers, such as oxygen isotopes, may be
566 a valuable step towards a more inclusive, global approach for tracing the provenance of
567 seafood.

568

569 **FUNDING** - Project was funded by an Australian Research Council Future Fellowship awarded
570 to Doubleday (FT190100244).

571 **DATA AVAILABILITY** – Data is available in supplementary information, except unpublished
572 data which is available from the corresponding authors upon reasonable request.

573 **DECLARATION OF INTERESTS** - The authors declare no competing interests.

574

5. TABLES

575
576
577
578
579
580
581
582
583
584
585
586

Table 1 – Confusion matrix of class classifications with percentage accuracies from random forest models, derived from a universal biomineral oxygen isoscape and isoscapes specific to statoliths of cephalopods, otoliths of fish, and exoskeleton shells of shellfish (bivalves and gastropods). This case study investigated whether samples can be classified back to region of origin between divergent climates and latitudes (Tropical Asia) or similar climates and latitudes (Temperate Asia, Temperate Australasia). Accurately classified samples are indicated in bold.

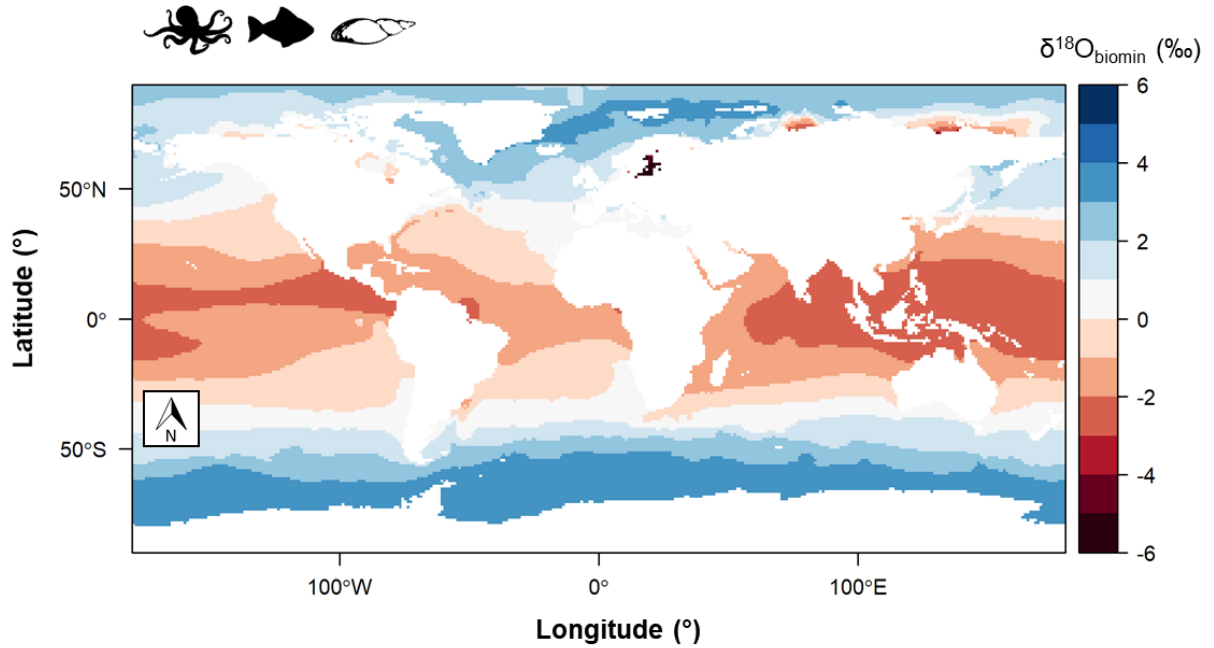
Isoscape	Predicted class	True class		
		Tropical Asia	Temperate Australasia	Temperate Asia
Universal biominerals	Tropical Asia	120	0	8
	Temperate Australasia	7	89	216
	Temperate Asia	286	26	345
	Class accuracy (%)	29.1	77.4	60.6
	Overall accuracy (%)			50.5
Cephalopod statoliths	Tropical Asia	8	0	0
	Temperate Australasia	10	10	0
	Temperate Asia	2	10	0
	Class accuracy (%)	40.0	50.0	-
	Overall accuracy (%)			45
Fish otoliths	Tropical Asia	185	0	8
	Temperate Australasia	1	25	0
	Temperate Asia	207	12	82
	Class accuracy (%)	47.1	67.6	91.1
	Overall accuracy (%)			63
Shellfish shells	Tropical Asia	0	0	0
	Temperate Australasia	0	30	176
	Temperate Asia	0	28	303
	Class accuracy (%)	-	51.7	63.3
	Overall accuracy (%)			62.0

587

6. FIGURES

588
589
590
591
592
593
594
595

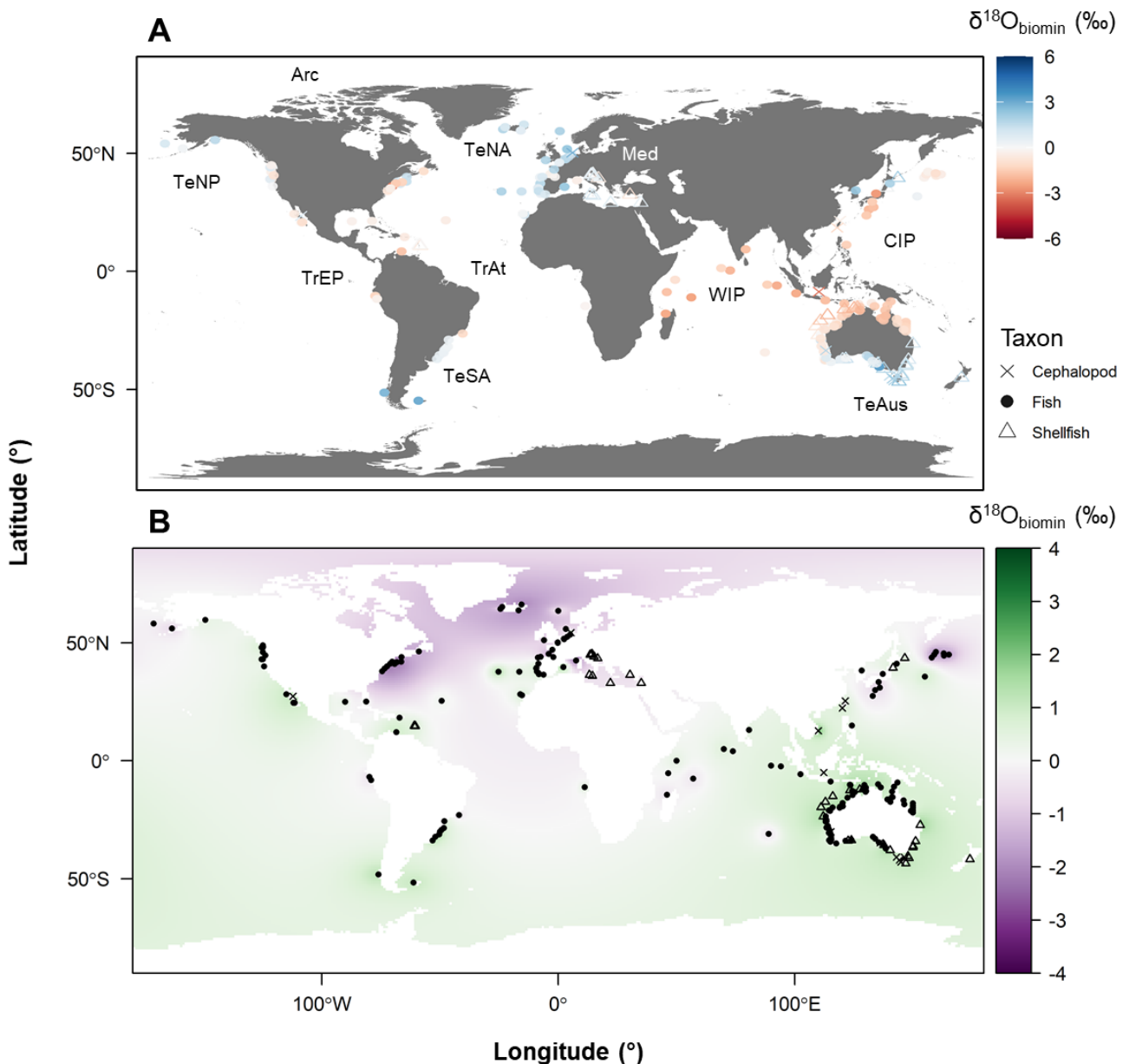
Figure 1 – Universal isoscape of predicted oxygen isotopes in biominerals ($\delta^{18}\text{O}_{\text{biomin}}$) of marine organisms. This isoscape represents an averaging of temperature-dependent fractionation equations of $\delta^{18}\text{O}_{\text{biomin}}$ from the statoliths of cephalopods, otoliths of fish, and exoskeleton shells of shellfish (bivalves and gastropods). Taxon-specific isoscapes are found in supplementary information (Figure S3).



596

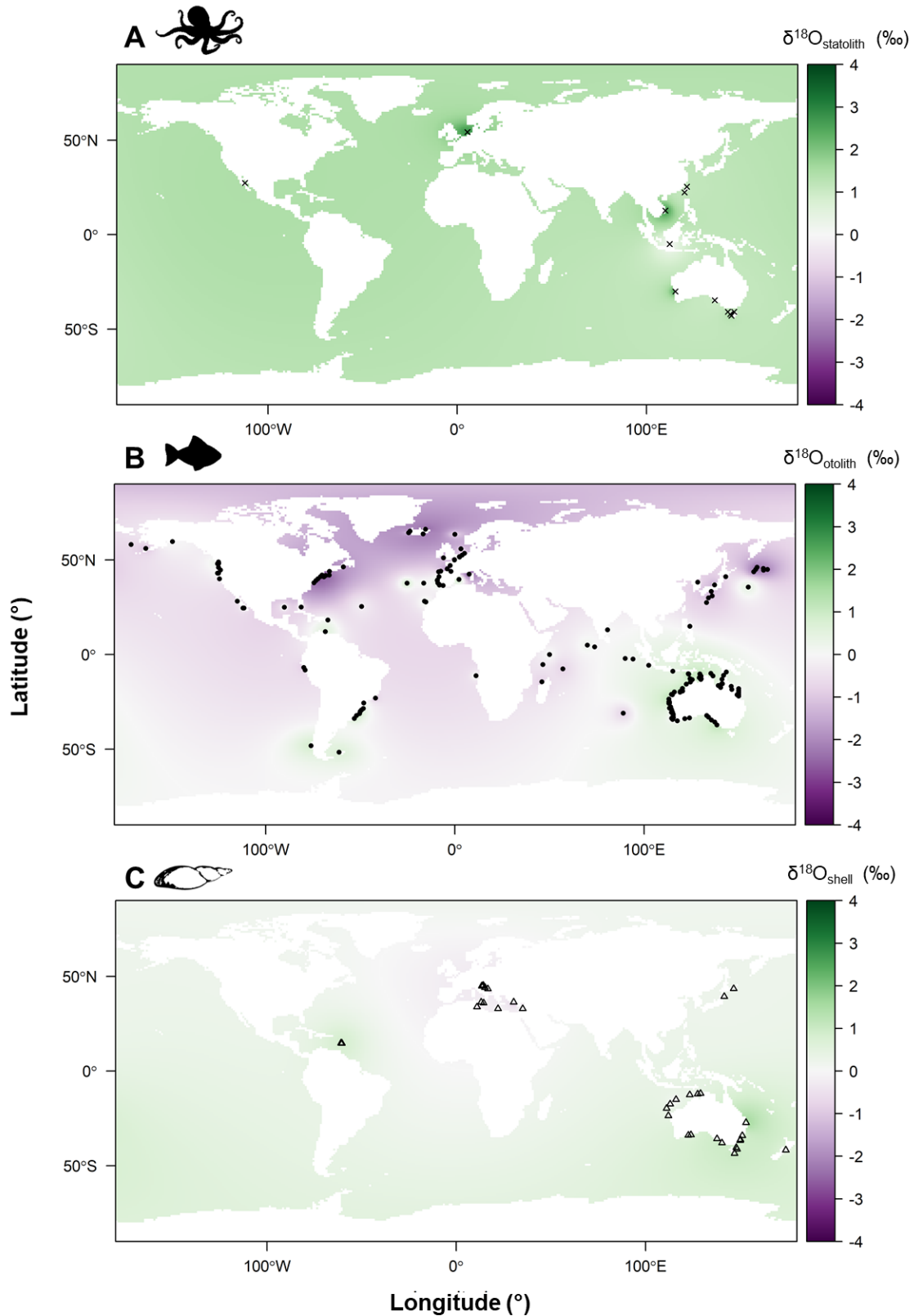
CONFIDENTIAL

597 **Figure 2** – Global maps representing A) measured oxygen isotopes ($\delta^{18}\text{O}_{\text{biomin}}$) values of geo-
 598 referenced samples (n = 3954, 68 species) from compiled database with ocean
 599 ecoregions labelled, and B) the residuals between measured and universal isoscape-
 600 derived predicted $\delta^{18}\text{O}_{\text{biomin}}$ values calculated per datapoint and then interpolated as a
 601 continuous surface onto a global map. The ocean ecoregions defined here include the
 602 Arctic (Arc), Temperate Northern Pacific (TeNP), Temperate Northern Atlantic (TeNA),
 603 Mediterranean (Med), Tropical Eastern Pacific (TrEP), Tropical Atlantic (TrAt), Central
 604 Indo-Pacific (CIP), Western Indo Pacific (WIP), Temperate Australasia (TeAus), and
 605 Temperate South America (TeSA) (Spalding et al., 2007).
 606

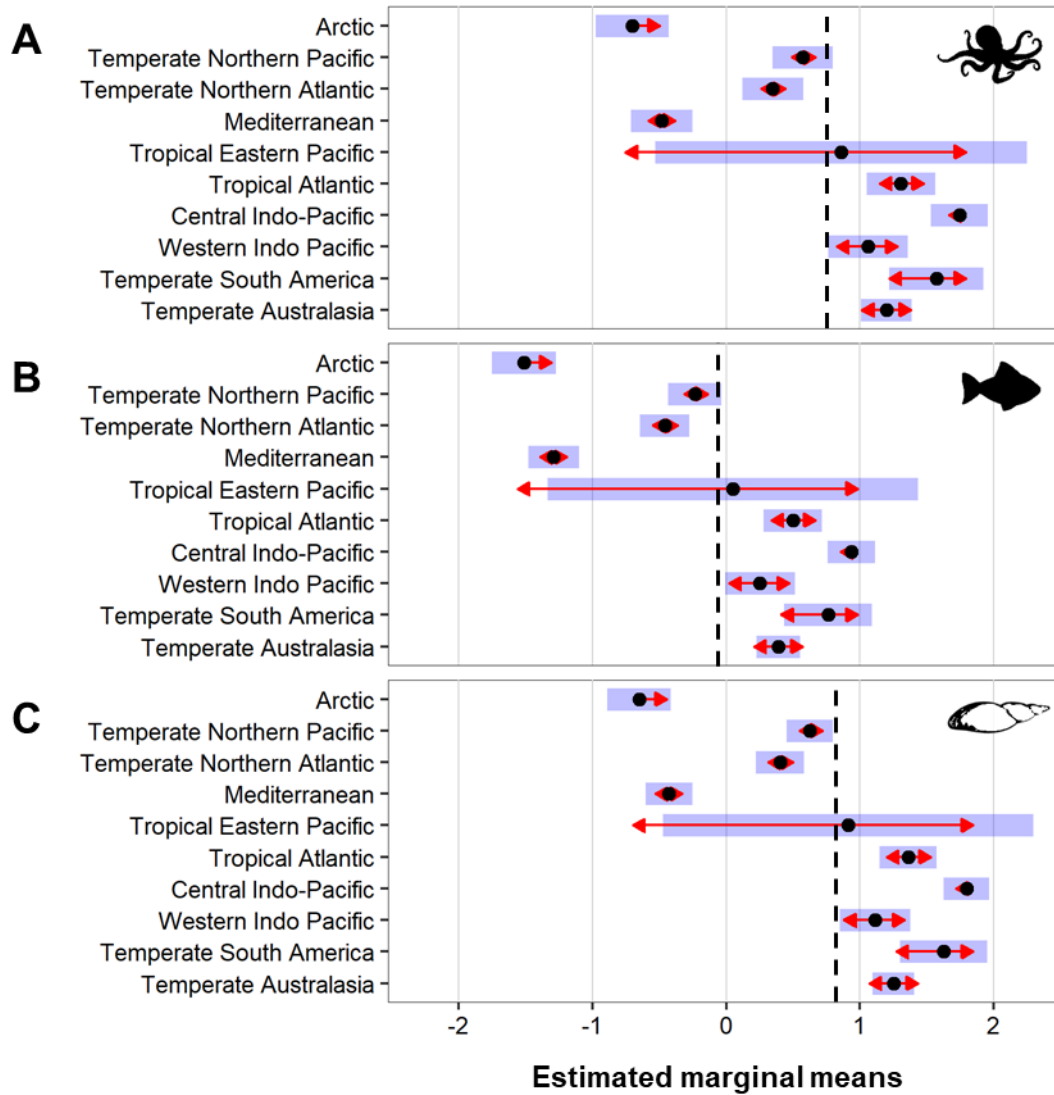


607

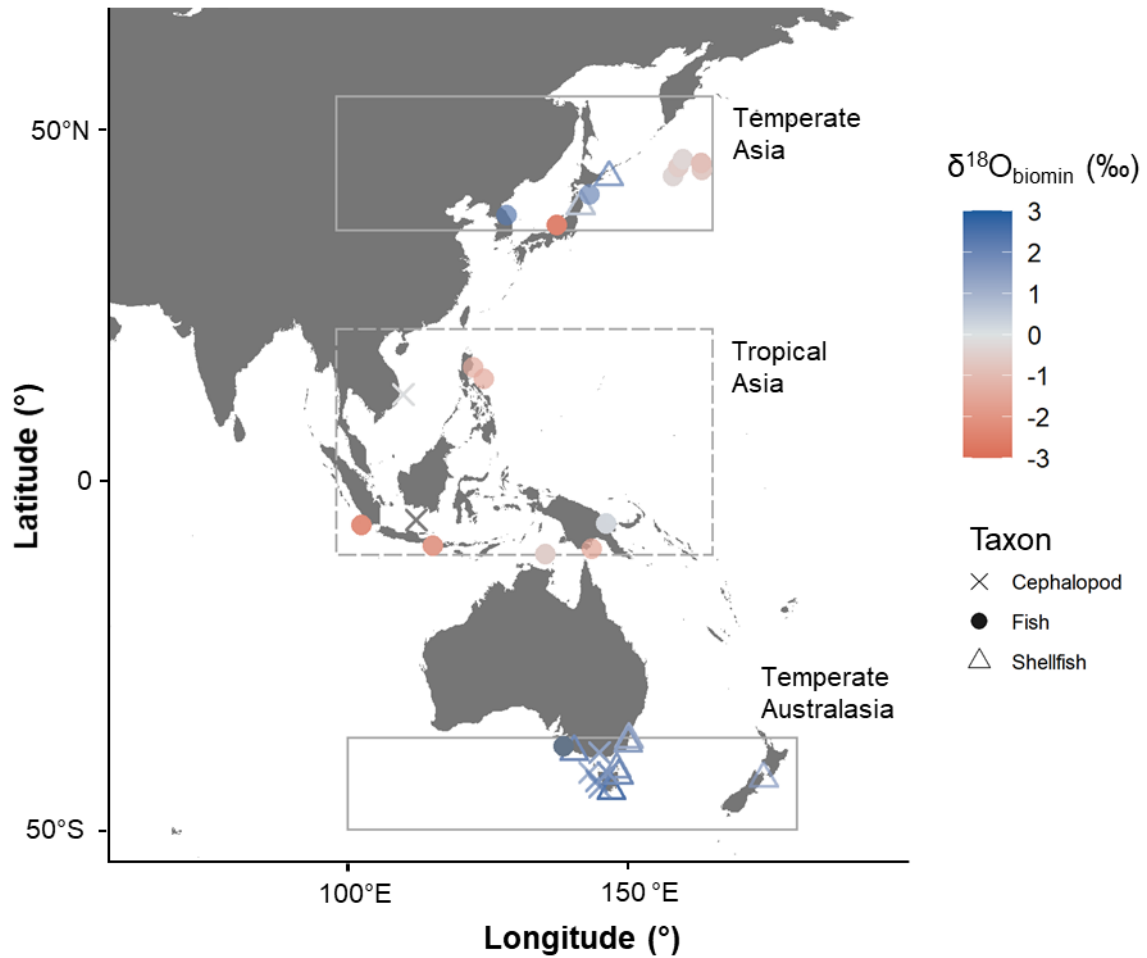
608 **Figure 3** – The residuals between measured and taxon-specific isoscape-derived predicted
609 oxygen isotope values in biominerals ($\delta^{18}\text{O}_{\text{biomin}}$) calculated per datapoint and then
610 interpolated as a continuous surface onto a global map for the A) statoliths of
611 cephalopods, B) otoliths of fish and C) exoskeleton shells of shellfish (bivalves and
612 gastropods).



613 **Figure 4** – Estimated marginal means of residuals between measured and universal isoscape-
 614 derived predicted oxygen isotope values in biominerals ($\delta^{18}\text{O}_{\text{biomin}}$) and separated into
 615 ocean bioregions and taxon of A) cephalopods B) fish, and C) shellfish. The bars
 616 indicate confidence intervals, whilst the red arrows are for comparisons between
 617 groups with overlaps across the horizontal axis indicating groups are not significantly
 618 different ($p > 0.05$). Dashed vertical lines indicate the estimated marginal mean of
 619 residuals averaged across regions for each taxon.
 620
 621



622 **Figure 5** – Measured oxygen isotope values ($n = 1097$, species = 16) in biominerals ($\delta^{18}\text{O}_{\text{biomin}}$)
623 of fish, shellfish, and cephalopods used in case-study to geolocate animals back to regions with climates and latitudes that are divergent (Tropical Asia) and similar
624 regions with climates and latitudes that are divergent (Tropical Asia) and similar
625 (Temperate Asia, Temperate Australasia). Also indicated are the boundary boxes of the
626 case study regions where predicted $\delta^{18}\text{O}_{\text{biomin}}$ values were extracted from isoscapes
627 and used to train random forest classification models.
628
629



7. REFERENCES

- 630
631
632 Artetxe-Arrate, I., Fraile, I., Farley, J., Darnaude, A. M., Clear, N., Dettman, D. L., Davies, C.,
633 Marsac, F., & Murua, H. (2021). Otolith $\delta^{18}\text{O}$ Composition as a Tracer of Yellowfin
634 Tuna (*Thunnus albacares*) Origin in the Indian Ocean. *Oceans*, 2(3), 461-476.
635 <https://www.mdpi.com/2673-1924/2/3/26>
636
637 Barendse, J., Roel, A., Longo, C., Andriessen, L., Webster, L. M. I., Ogden, R., & Neat, F.
638 (2019, 2019/03/18/). DNA barcoding validates species labelling of certified seafood.
639 *Current Biology*, 29(6), R198-R199.
640 <https://doi.org/https://doi.org/10.1016/j.cub.2019.02.014>
641
642 Bath, G. E., Thorrold, S. R., Jones, C. M., Campana, S. E., McLaren, J. W., & Lam, J. W.
643 (2000). Strontium and barium uptake in aragonitic otoliths of marine fish. *Geochimica*
644 *et Cosmochimica Acta*, 64(10), 1705-1714.
645 [https://doi.org/https://doi.org/10.1016/S0016-7037\(99\)00419-6](https://doi.org/https://doi.org/10.1016/S0016-7037(99)00419-6)
646
647 Bernatchez, L., Wellenreuther, M., Araneda, C., Ashton, D. T., Barth, J. M. I., Beacham, T.
648 D., Maes, G. E., Martinsohn, J. T., Miller, K. M., Naish, K. A., Ovenden, J. R.,
649 Primmer, C. R., Young Suk, H., Therkildsen, N. O., & Withler, R. E. (2017,
650 2017/09/01/). Harnessing the Power of Genomics to Secure the Future of Seafood.
651 *Trends in Ecology & Evolution*, 32(9), 665-680.
652 <https://doi.org/https://doi.org/10.1016/j.tree.2017.06.010>
653
654 Bryant, J. D., Koch, P. L., Froelich, P. N., Showers, W. J., & Genna, B. J. (1996). Oxygen
655 isotope partitioning between phosphate and carbonate in mammalian apatite.
656 *Geochimica et Cosmochimica Acta*, 60(24), 5145-5148.
657
658 Burnham, K. P., & Anderson, D. R. (2004). Multimodel inference: understanding AIC and
659 BIC in model selection. *Sociological methods & research*, 33(2), 261-304.
660
661 Caldarescu, D. E., Sadatzki, H., Andersson, C., Schäfer, P., Fortunato, H., & Meckler, A. N.
662 (2021, 2021/02/01/). Clumped isotope thermometry in bivalve shells: A tool for
663 reconstructing seasonal upwelling. *Geochimica et Cosmochimica Acta*, 294, 174-
664 191. <https://doi.org/https://doi.org/10.1016/j.gca.2020.11.019>
665
666 Calosso, M. C., Claydon, J. A., Mariani, S., & Cawthorn, D.-M. (2020). Global footprint of
667 mislabelled seafood on a small island nation. *Biological Conservation*, 245, 108557.
668
669 Camin, F., Bontempo, L., Perini, M., & Piasentier, E. (2016). Stable isotope ratio analysis for
670 assessing the authenticity of food of animal origin. *Comprehensive Reviews in Food*
671 *Science and Food Safety*, 15(5), 868-877. [https://doi.org/doi:10.1111/1541-](https://doi.org/doi:10.1111/1541-4337.12219)
672 [4337.12219](https://doi.org/doi:10.1111/1541-4337.12219)
673
674 Cazelles, K., Zemlak, T. S., Gutgesell, M., Myles-Gonzalez, E., Hanner, R., & Shear
675 McCann, K. (2021). Spatial Fingerprinting: Horizontal Fusion of Multi-Dimensional
676 Bio-Tracers as Solution to Global Food Provenance Problems. *Foods*, 10(4), 717.
677 <https://www.mdpi.com/2304-8158/10/4/717>
678
679 Chung, M.-T., Chen, C.-Y., Shiao, J.-C., Lin, S., & Wang, C.-H. (2020, 2020/08/01/).
680 Temperature-dependent fractionation of stable oxygen isotopes differs between
681 cuttlefish statoliths and cuttlebones. *Ecological Indicators*, 115, 106457.
682 <https://doi.org/https://doi.org/10.1016/j.ecolind.2020.106457>
683

- 684 Chung, M.-T., Chen, C.-Y., Shiao, J.-C., Shirai, K., & Wang, C.-H. (2021). Metabolic proxy
685 for cephalopods: Stable carbon isotope values recorded in different biogenic
686 carbonates. *Methods in Ecology and Evolution*.
687
- 688 Chung, M.-T., Trueman, C. N., Godiksen, J. A., Holmstrup, M. E., & Grønkjær, P. (2019).
689 Field metabolic rates of teleost fishes are recorded in otolith carbonate.
690 *Communications biology*, 2(1), 1-10.
691
- 692 Conroy, J. L., Cobb, K. M., Lynch-Stieglitz, J., & Polissar, P. J. (2014). Constraints on the
693 salinity–oxygen isotope relationship in the central tropical Pacific Ocean. *Marine*
694 *Chemistry*, 161, 26-33.
695
- 696 Costas-Rodríguez, M., Lavilla, I., & Bendicho, C. (2010). Classification of cultivated mussels
697 from Galicia (Northwest Spain) with European Protected Designation of Origin using
698 trace element fingerprint and chemometric analysis. *Analytica chimica acta*, 664(2),
699 121-128.
700
- 701 Craig, H., & Gordon, L. I. (1965). Deuterium and oxygen 18 variations in the ocean and the
702 marine atmosphere.
703
- 704 Cusa, M., St John Glew, K., Trueman, C., Mariani, S., Buckley, L., Neat, F., & Longo, C.
705 (2021, 2021/09/13). A future for seafood point-of-origin testing using DNA and stable
706 isotope signatures. *Reviews in Fish Biology and Fisheries*.
707 <https://doi.org/10.1007/s11160-021-09680-w>
708
- 709 Cusa, M., St John Glew, K., Trueman, C., Mariani, S., Buckley, L., Neat, F., & Longo, C.
710 (2022). A future for seafood point-of-origin testing using DNA and stable isotope
711 signatures. *Reviews in Fish Biology and Fisheries*, 32(2), 597-621.
712
- 713 Duarte, B., Duarte, I. A., Caçador, I., Reis-Santos, P., Vasconcelos, R. P., Gameiro, C.,
714 Tanner, S. E., & Fonseca, V. F. (2022). Elemental fingerprinting of thornback ray
715 (*Raja clavata*) muscle tissue as a tracer for provenance and food safety assessment.
716 *Food Control*, 133, 108592.
717
- 718 Fox, M., Mitchell, M., Dean, M., Elliott, C., & Campbell, K. (2018). The seafood supply chain
719 from a fraudulent perspective. *Food Security*, 10(4), 939-963.
720
- 721 Geffen, A. J. (2012). Otolith oxygen and carbon stable isotopes in wild and laboratory-reared
722 plaice (*Pleuronectes platessa*). *Environmental Biology of Fishes*, 95(4), 419-430.
723
- 724 Godiksen, J. A., Svenning, M.-A., Dempson, J. B., Marttila, M., Storm-Suke, A., & Power, M.
725 (2010). Development of a species-specific fractionation equation for Arctic charr
726 (*Salvelinus alpinus* (L.)): an experimental approach. *Hydrobiologia*, 650(1), 67-77.
727 <https://doi.org/https://doi.org/10.1007/s10750-009-0056-7>
728
- 729 Gopi, K., Mazumder, D., Sammut, J., & Saintilan, N. (2019). Determining the provenance
730 and authenticity of seafood: A review of current methodologies. *Trends in Food*
731 *Science & Technology*, 91, 294-304.
732
- 733 Graham, J. B., & Dickson, K. A. (2004). Tuna comparative physiology. *Journal of*
734 *Experimental Biology*, 207(23), 4015-4024. <https://doi.org/10.1242/jeb.01267>
735
- 736 Grammer, G. L., Morrongiello, J. R., Izzo, C., Hawthorne, P. J., Middleton, J. F., &
737 Gillanders, B. M. (2017). Coupling biogeochemical tracers with fish growth reveals

738 physiological and environmental controls on otolith chemistry. *Ecological*
739 *Monographs*, 87(3), 487-507.

740

741 Grömping, U. (2006). Relative importance for linear regression in R: the package relaimpo.
742 *Journal of statistical software*, 17(1), 1-27.

743

744 Grossman, E. L., & Ku, T.-L. (1986, 1986/01/01/). Oxygen and carbon isotope fractionation
745 in biogenic aragonite: Temperature effects. *Chemical Geology: Isotope Geoscience*
746 *section*, 59, 59-74. [https://doi.org/https://doi.org/10.1016/0168-9622\(86\)90057-6](https://doi.org/https://doi.org/10.1016/0168-9622(86)90057-6)

747

748 Hane, Y., Kimura, S., Yokoyama, Y., Miyairi, Y., Ushikubo, T., Ishimura, T., Ogawa, N.,
749 Aono, T., & Nishida, K. (2020). Reconstruction of temperature experienced by Pacific
750 bluefin tuna *Thunnus orientalis* larvae using SIMS and microvolume CF-IRMS otolith
751 oxygen isotope analyses. *Marine Ecology Progress Series*, 649, 175-188.

752

753 Hijmans, R. J., Van Etten, J., Cheng, J., Mattiuzzi, M., Sumner, M., Greenberg, J. A.,
754 Lamigueiro, O. P., Bevan, A., Racine, E. B., & Shortridge, A. (2015). Package
755 'raster'. *R package*, 734.

756

757 Høie, H., Otterlei, E., & Folkvord, A. (2004). Temperature-dependent fractionation of stable
758 oxygen isotopes in otoliths of juvenile cod (*Gadus morhua* L.). *ICES Journal of*
759 *Marine Science*, 61(2), 243-251.

760

761 Howson, P. (2020). Building trust and equity in marine conservation and fisheries supply
762 chain management with blockchain. *Marine Policy*, 115, 103873.

763

764 Hudson, J., & Anderson, T. (1989). Ocean temperatures and isotopic compositions through
765 time. *Earth and Environmental Science Transactions of the Royal Society of*
766 *Edinburgh*, 80(3-4), 183-192.

767

768 Hüssy, K., Limburg, K. E., de Pontual, H., Thomas, O. R., Cook, P. K., Heimbrand, Y., Blass,
769 M., & Sturrock, A. M. (2021). Trace element patterns in otoliths: the role of
770 biomineralization. *Reviews in Fisheries Science & Aquaculture*, 29(4), 445-477.

771

772 Jacquet, J. L., & Pauly, D. (2008, 2008/05/01/). Trade secrets: Renaming and mislabeling of
773 seafood. *Marine Policy*, 32(3), 309-318.
774 <https://doi.org/https://doi.org/10.1016/j.marpol.2007.06.007>

775

776 Jeandel, C., Arsouze, T., Lacan, F., Techine, P., & Dutay, J.-C. (2007). Isotopic Nd
777 compositions and concentrations of the lithogenic inputs into the ocean: A
778 compilation, with an emphasis on the margins. *Chemical Geology*, 239(1-2), 156-
779 164.

780

781 Kalish, J. M. (1991). ^{13}C and ^{18}O isotopic disequilibria in fish otoliths: metabolic and kinetic
782 effects. *Marine Ecology Progress Series*, 75(2-3), 191-203.

783

784 Kelly, S., Heaton, K., & Hoogewerff, J. (2005, 2005/12/01/). Tracing the geographical origin
785 of food: The application of multi-element and multi-isotope analysis. *Trends in Food*
786 *Science & Technology*, 16(12), 555-567.
787 <https://doi.org/https://doi.org/10.1016/j.tifs.2005.08.008>

788

789 Kim, S.-T., O'Neil, J. R., Hillaire-Marcel, C., & Mucci, A. (2007, 2007/10/01/). Oxygen isotope
790 fractionation between synthetic aragonite and water: Influence of temperature and
791 Mg^{2+} concentration. *Geochimica et Cosmochimica Acta*, 71(19), 4704-4715.
792 <https://doi.org/https://doi.org/10.1016/j.gca.2007.04.019>

793
794 Kitagawa, T., Ishimura, T., Uozato, R., Shirai, K., Amano, Y., Shinoda, A., Otake, T.,
795 Tsunogai, U., & Kimura, S. (2013). Otolith $\delta^{18}\text{O}$ of Pacific bluefin tuna *Thunnus*
796 *orientalis* as an indicator of ambient water temperature. *Marine Ecology Progress*
797 *Series*, 481, 199-209.
798
799 Kitagawa, T., Kimura, S., Nakata, H., & Yamada, H. (2006). Thermal adaptation of Pacific
800 bluefin tuna *Thunnus orientalis* to temperate waters. *Fisheries Science*, 72(1), 149-
801 156.
802
803 Kittinger, J. N., Teh, L. C., Allison, E. H., Bennett, N. J., Crowder, L. B., Finkbeiner, E. M.,
804 Hicks, C., Scarton, C. G., Nakamura, K., & Ota, Y. (2017). Committing to socially
805 responsible seafood. *Science*, 356(6341), 912-913.
806
807 Kolding, J., Béné, C., & Bavinck, M. (2014). Small-scale fisheries: Importance, vulnerability
808 and deficient knowledge. *Governance of marine fisheries and biodiversity*
809 *conservation: Interaction and coevolution*, 317-331.
810
811 Kompas, T., Grafton, R. Q., & Che, T. N. (2010). Bioeconomic losses from overharvesting
812 tuna. *Conservation Letters*, 3(3), 177-183.
813 <https://doi.org/https://doi.org/10.1111/j.1755-263X.2010.00103.x>
814
815 Lamigueiro, O. P., Hijmans, R., & Lamigueiro, M. O. P. (2022). Package 'rasterVis'.
816
817 Lécuyer, C., Hutzler, A., Amiot, R., Daux, V., Grosheny, D., Otero, O., Martineau, F., Fourel,
818 F., Balter, V., & Reynard, B. (2012, 2012/11/25/). Carbon and oxygen isotope
819 fractionations between aragonite and calcite of shells from modern molluscs.
820 *Chemical Geology*, 332-333, 92-101.
821 <https://doi.org/https://doi.org/10.1016/j.chemgeo.2012.08.034>
822
823 LeGrande, A. N., & Schmidt, G. A. (2006). Global gridded data set of the oxygen isotopic
824 composition in seawater. *Geophysical research letters*, 33(12).
825 <https://doi.org/https://doi.org/10.1029/2006GL026011>
826
827 Lenth, R., Singmann, H., Love, J., Buerkner, P., & Herve, M. (2018). Emmeans: Estimated
828 marginal means, aka least-squares means. *R package version*, 1(1), 3.
829
830 Li, L., Boyd, C. E., & Sun, Z. (2016). Authentication of fishery and aquaculture products by
831 multi-element and stable isotope analysis. *Food Chemistry*, 194, 1238-1244.
832
833 Liaw, A., & Wiener, M. (2002). Classification and regression by randomForest. *R news*, 2(3),
834 18-22.
835
836 Lindley, J. (2020). Food security amidst crime: harm of illegal fishing and fish fraud on
837 sustainable oceans. *The Palgrave Handbook of Climate Resilient Societies*, 1-19.
838
839 Lindley, J. (2021). Food security amidst crime: harm of illegal fishing and fish fraud on
840 sustainable oceans. In R. Brears (Ed.), *The Palgrave Handbook of Climate Resilient*
841 *Societies*. Palgrave Macmillan. [https://doi.org/https://doi.org/10.1007/978-3-030-](https://doi.org/https://doi.org/10.1007/978-3-030-32811-5_127-1)
842 [32811-5_127-1](https://doi.org/https://doi.org/10.1007/978-3-030-32811-5_127-1)
843
844 Luquet, G. (2012). Biomineralizations: insights and prospects from crustaceans.
845 *ZooKeys*(176), 103-121. <https://doi.org/10.3897/zookeys.176.2318>
846

- 847 Macdonald, J. I., Drysdale, R. N., Witt, R., Cságyó, Z., & Marteinsdóttir, G. (2020,
848 2020/03/01). Isolating the influence of ontogeny helps predict island-wide variability
849 in fish otolith chemistry. *Reviews in Fish Biology and Fisheries*, 30(1), 173-202.
850 <https://doi.org/10.1007/s11160-019-09591-x>
851
- 852 Madigan, D. J., Carlisle, A. B., Gardner, L. D., Jayasundara, N., Micheli, F., Schaefer, K. M.,
853 Fuller, D. W., & Block, B. A. (2015). Assessing niche width of endothermic fish from
854 genes to ecosystem. *Proceedings of the National Academy of Sciences*, 112(27),
855 8350-8355.
856
- 857 Malik, A., Dickson, K. A., Kitagawa, T., Fujioka, K., Estess, E. E., Farwell, C., Forsgren, K.,
858 Bush, J., & Schuller, K. A. (2020, 2020/08/27). Ontogeny of regional endothermy in
859 Pacific bluefin tuna (*Thunnus orientalis*). *Marine Biology*, 167(9), 133.
860 <https://doi.org/10.1007/s00227-020-03753-3>
861
- 862 Martino, J. C., Doubleday, Z. A., Chung, M.-T., & Gillanders, B. M. (2020). Experimental
863 support towards a metabolic proxy in fish using otolith carbon isotopes. *Journal of*
864 *Experimental Biology*, 223(6), jeb217091.
865
- 866 Martino, J. C., Doubleday, Z. A., Fowler, A. J., & Gillanders, B. M. (2021). Identifying
867 physiological and environmental influences on otolith chemistry in a coastal fishery
868 species. *Marine and Freshwater Research*, 72(6), 922-924.
869 https://doi.org/https://doi.org/10.1071/MF20196_CO
870
- 871 Martino, J. C., Mazumder, D., Gadd, P., & Doubleday, Z. A. (2022). Tracking the provenance
872 of octopus using isotopic and multi-elemental analysis. *Food Chemistry*, 371,
873 1311133.
874
- 875 Martinsohn, J. T., Raymond, P., Knott, T., Glover, K. A., Nielsen, E. E., Eriksen, L. B.,
876 Ogden, R., Casey, J., & Guillen, J. (2019). DNA-analysis to monitor fisheries and
877 aquaculture: Too costly? *Fish and Fisheries*, 20(2), 391-401.
878
- 879 Merchant, C. J., Embury, O., Bulgin, C. E., Block, T., Corlett, G. K., Fiedler, E., Good, S. A.,
880 Mittaz, J., Rayner, N. A., Berry, D., Eastwood, S., Taylor, M., Tsushima, Y., Waterfall,
881 A., Wilson, R., & Donlon, C. (2019, 2019/10/22). Satellite-based time-series of sea-
882 surface temperature since 1981 for climate applications. *Scientific Data*, 6(1), 223.
883 <https://doi.org/10.1038/s41597-019-0236-x>
884
- 885 Monahan, F. J., Schmidt, O., & Moloney, A. P. (2018). Meat provenance: Authentication of
886 geographical origin and dietary background of meat. *Meat science*, 144, 2-14.
887
- 888 Nakamura, M., Yoneda, M., Ishimura, T., Shirai, K., Tamamura, M., & Nishida, K. (2020).
889 Temperature dependency equation for chub mackerel *Scomber japonicus* identified
890 by a laboratory rearing experiment and microscale analysis. *Marine and Freshwater*
891 *Research*, 71(10), 1384-1389. <https://doi.org/https://doi.org/10.1071/MF19313>
892
- 893 Nishida, K., Suzuki, A., Isono, R., Hayashi, M., Watanabe, Y., Yamamoto, Y., Irie, T., Nojiri,
894 Y., Mori, C., & Sato, M. (2015). Thermal dependency of shell growth, microstructure,
895 and stable isotopes in laboratory-reared *Scapharca broughtonii* (Mollusca: Bivalvia).
896 *Geochemistry, Geophysics, Geosystems*, 16(7), 2395-2408.
897 <https://doi.org/https://doi.org/10.1002/2014GC005634>
898
- 899 Owen, E. F., Wanamaker Jr, A. D., Feindel, S. C., Schöne, B. R., & Rawson, P. D. (2008).
900 Stable carbon and oxygen isotope fractionation in bivalve (*Placopecten*

901 *magellanicus*) larval aragonite. *Geochimica et Cosmochimica Acta*, 72(19), 4687-
902 4698. <https://doi.org/https://doi.org/10.1016/j.gca.2008.06.029>
903
904 Pearson, R. M., van de Merwe, J. P., & Connolly, R. M. (2020). Global oxygen isoscapes for
905 barnacle shells: application for tracing movement in oceans. *Science of The Total*
906 *Environment*, 705, 135782.
907
908 Pebesma, E. J. (2004). Multivariable geostatistics in S: the gstat package. *Computers &*
909 *geosciences*, 30(7), 683-691.
910
911 Radtke, R., Lenz, P., Showers, W., & Moksness, E. (1996). Environmental information
912 stored in otoliths: insights from stable isotopes. *Marine Biology*, 127(1), 161-170.
913 <https://doi.org/https://doi.org/10.1007/BF00993656>
914
915 Rasmussen, R. S., & Morrissey, M. T. (2008). DNA-based methods for the identification of
916 commercial fish and seafood species. *Comprehensive reviews in food science and*
917 *food safety*, 7(3), 280-295.
918
919 Saitoh, Y., Nakano, T., Shin, K. C., Matsubayashi, J., Kato, Y., Amakawa, H., Osada, Y.,
920 Yoshimizu, C., Okuda, N., & Amano, Y. (2018). Utility of Nd isotope ratio as a tracer
921 of marine animals: regional variation in coastal seas and causal factors. *Ecosphere*,
922 9(8), e02365.
923
924 Sakamoto, T., Komatsu, K., Shirai, K., Higuchi, T., Ishimura, T., Setou, T., Kamimura, Y.,
925 Watanabe, C., & Kawabata, A. (2019). Combining microvolume isotope analysis and
926 numerical simulation to reproduce fish migration history. *Methods in Ecology and*
927 *Evolution*, 10(1), 59-69. <https://doi.org/https://doi.org/10.1111/2041-210X.13098>
928
929 Sakamoto, T., Komatsu, K., Yoneda, M., Ishimura, T., Higuchi, T., Shirai, K., Kamimura, Y.,
930 Watanabe, C., & Kawabata, A. (2017). Temperature dependence of $\delta^{18}\text{O}$ in otolith of
931 juvenile Japanese sardine: laboratory rearing experiment with micro-scale analysis.
932 *Fisheries Research*, 194, 55-59.
933
934 Shirai, K., Otake, T., Amano, Y., Kuroki, M., Ushikubo, T., Kita, N. T., Murayama, M.,
935 Tsukamoto, K., & Valley, J. W. (2018). Temperature and depth distribution of
936 Japanese eel eggs estimated using otolith oxygen stable isotopes. *Geochimica et*
937 *Cosmochimica Acta*, 236, 373-383.
938
939 Singh, A., Jani, R., & Ramesh, R. (2010). Spatiotemporal variations of the $\delta^{18}\text{O}$ -salinity
940 relation in the northern Indian Ocean. *Deep Sea Research Part I: Oceanographic*
941 *Research Papers*, 57(11), 1422-1431.
942
943 Soares, S., Amaral, J. S., Oliveira, M. B. P., & Mafra, I. (2017). A comprehensive review on
944 the main honey authentication issues: Production and origin. *Comprehensive*
945 *Reviews in Food Science and Food Safety*, 16(5), 1072-1100.
946
947 Spalding, M. D., Fox, H. E., Allen, G. R., Davidson, N., Ferdaña, Z. A., Finlayson, M.,
948 Halpern, B. S., Jorge, M. A., Lombana, A., & Lourie, S. A. (2007). Marine ecoregions
949 of the world: a bioregionalization of coastal and shelf areas. *BioScience*, 57(7), 573-
950 583.
951
952 Stock, C. A., John, J. G., Rykaczewski, R. R., Asch, R. G., Cheung, W. W. L., Dunne, J. P.,
953 Friedland, K. D., Lam, V. W. Y., Sarmiento, J. L., & Watson, R. A. (2017).
954 Reconciling fisheries catch and ocean productivity. *Proceedings of the National*

955 *Academy of Sciences*, 114(8), E1441-E1449.
 956 <https://doi.org/doi:10.1073/pnas.1610238114>
 957
 958 Tanaka, K., Zhao, L., Tazoe, H., Iizuka, T., Murakami-Sugihara, N., Toyama, K., Yamamoto,
 959 T., Yorisue, T., & Shirai, K. (2022, 2022/07/15/). Using neodymium isotope ratio in
 960 *Ruditapes philippinarum* shells for tracking the geographical origin. *Food Chemistry*,
 961 382, 131914. <https://doi.org/https://doi.org/10.1016/j.foodchem.2021.131914>
 962
 963 Team, R. C. (2013). R development core team. *RA Lang Environ Stat Comput*, 55, 275-286.
 964
 965 Thorrold, S. R., Campana, S. E., Jones, C. M., & Swart, P. K. (1997). Factors determining
 966 $\delta^{13}\text{C}$ and $\delta^{18}\text{O}$ fractionation in aragonitic otoliths of marine fish. *Geochimica et*
 967 *Cosmochimica Acta*, 61(14), 2909-2919.
 968
 969 Trueman, C. N., & Glew, K. S. J. (2019). Isotopic tracking of marine animal movement. In
 970 *Tracking animal migration with stable isotopes* (pp. 137-172). Elsevier.
 971
 972 Trueman, C. N., MacKenzie, K., & Palmer, M. (2012). Identifying migrations in marine fishes
 973 through stable-isotope analysis. *Journal of Fish Biology*, 81(2), 826-847.
 974
 975 van Ruth, S. M., Huisman, W., & Luning, P. A. (2017). Food fraud vulnerability and its key
 976 factors. *Trends in Food Science & Technology*, 67, 70-75.
 977
 978 Voelker, A. H. L., Colman, A., Olack, G., Waniek, J. J., & Hodell, D. (2015, 2015/06/01/).
 979 Oxygen and hydrogen isotope signatures of Northeast Atlantic water masses. *Deep*
 980 *Sea Research Part II: Topical Studies in Oceanography*, 116, 89-106.
 981 <https://doi.org/https://doi.org/10.1016/j.dsr2.2014.11.006>
 982
 983 Walther, B. D., & Thorrold, S. R. (2006). Water, not food, contributes the majority of
 984 strontium and barium deposited in the otoliths of a marine fish. *Marine Ecology*
 985 *Progress Series*, 311, 125-130. <https://doi.org/10.3354/meps311125>
 986
 987 Wanamaker Jr, A. D., Kreutz, K. J., Borns Jr, H. W., Introne, D. S., Feindel, S., Funder, S.,
 988 Rawson, P. D., & Barber, B. J. (2007). Experimental determination of salinity,
 989 temperature, growth, and metabolic effects on shell isotope chemistry of *Mytilus*
 990 *edulis* collected from Maine and Greenland. *Paleoceanography*, 22(2).
 991 <https://doi.org/https://doi.org/10.1029/2006PA001352>
 992
 993 Wickham, H. (2011). ggplot2. *Wiley Interdisciplinary Reviews: Computational Statistics*, 3(2),
 994 180-185.
 995
 996 Zachos, J. C., Stott, L. D., & Lohmann, K. C. (1994). Evolution of Early Cenozoic marine
 997 temperatures. *Paleoceanography*, 9(2), 353-387.
 998 <https://doi.org/https://doi.org/10.1029/93PA03266>
 999
 1000 Zhao, L., Tanaka, K., Tazoe, H., Iizuka, T., Kubota, K., Murakami-Sugihara, N., & Shirai, K.
 1001 (2019). Determination of the geographical origin of marine mussels (*Mytilus* spp.)
 1002 using $^{143}\text{Nd}/^{144}\text{Nd}$ ratios. *Marine environmental research*, 148, 12-18.
 1003
 1004